

**Dipolar Spin Ice States with a Fast Monopole Hopping Rate in  $\text{CdEr}_2\text{X}_4$  ( $X = \text{Se}, \text{S}$ )**

Shang Gao,<sup>1,2</sup> O. Zaharko,<sup>1,\*</sup> V. Tsurkan,<sup>3,4</sup> L. Prodan,<sup>4</sup> E. Riordan,<sup>5</sup> J. Lago,<sup>6</sup> B. Fåk,<sup>7</sup> A. R. Wildes,<sup>7</sup> M. M. Koza,<sup>7</sup> C. Ritter,<sup>7</sup> P. Fouquet,<sup>7</sup> L. Keller,<sup>1</sup> E. Canévet,<sup>1,11</sup> M. Medarde,<sup>8</sup> J. Blomgren,<sup>9</sup> C. Johansson,<sup>9</sup> S. R. Giblin,<sup>5</sup> S. Vrtnik,<sup>10</sup> J. Luzar,<sup>10</sup> A. Loidl,<sup>3</sup> Ch. Rüegg,<sup>1,2</sup> and T. Fennell<sup>1,†</sup>

<sup>1</sup>Laboratory for Neutron Scattering and Imaging, Paul Scherrer Institut, CH-5232 Villigen PSI, Switzerland

<sup>2</sup>Department of Quantum Matter Physics, University of Geneva, CH-1211 Geneva, Switzerland

<sup>3</sup>Experimental Physics V, University of Augsburg, D-86135 Augsburg, Germany

<sup>4</sup>Institute of Applied Physics, Academy of Sciences of Moldova, MD-2028 Chisinau, Republic of Moldova

<sup>5</sup>School of Physics and Astronomy, Cardiff University, CF24 3AA Cardiff, United Kingdom

<sup>6</sup>Department of Inorganic Chemistry, Universidad del País Vasco (UPV-EHU), 48080 Bilbao, Spain

<sup>7</sup>Institut Laue-Langevin, CS 20156, 38042 Grenoble Cedex 9, France

<sup>8</sup>Laboratory for Scientific Developments and Novel Materials, Paul Scherrer Institut, CH-5232 Villigen PSI, Switzerland

<sup>9</sup>RISE Acreo AB, SE-411 33 Göteborg, Sweden

<sup>10</sup>Jožef Stefan Institute, SI-1000 Ljubljana, Slovenia

<sup>11</sup>Department of Physics, Technical University of Denmark, DK-2800 Kgs. Lyngby, Denmark



(Received 30 May 2017; published 30 March 2018)

Excitations in a spin ice behave as magnetic monopoles, and their population and mobility control the dynamics of a spin ice at low temperature.  $\text{CdEr}_2\text{Se}_4$  is reported to have the Pauling entropy characteristic of a spin ice, but its dynamics are three orders of magnitude faster than the canonical spin ice  $\text{Dy}_2\text{Ti}_2\text{O}_7$ . In this Letter we use diffuse neutron scattering to show that both  $\text{CdEr}_2\text{Se}_4$  and  $\text{CdEr}_2\text{S}_4$  support a dipolar spin ice state—the host phase for a Coulomb gas of emergent magnetic monopoles. These Coulomb gases have similar parameters to those in  $\text{Dy}_2\text{Ti}_2\text{O}_7$ , i.e., dilute and uncorrelated, and so cannot provide three orders faster dynamics through a larger monopole population alone. We investigate the monopole dynamics using ac susceptometry and neutron spin echo spectroscopy, and verify the crystal electric field Hamiltonian of the  $\text{Er}^{3+}$  ions using inelastic neutron scattering. A quantitative calculation of the monopole hopping rate using our Coulomb gas and crystal electric field parameters shows that the fast dynamics in  $\text{CdEr}_2\text{X}_4$  ( $X = \text{Se}, \text{S}$ ) are primarily due to much faster monopole hopping. Our work suggests that  $\text{CdEr}_2\text{X}_4$  offer the possibility to study alternative spin ice ground states and dynamics, with equilibration possible at much lower temperatures than the rare earth pyrochlore examples.

DOI: [10.1103/PhysRevLett.120.137201](https://doi.org/10.1103/PhysRevLett.120.137201)

A magnetic Coulomb phase is characterized by an effective magnetic field whose topological defects behave as emergent magnetic monopoles [1]. In dipolar spin ices such as  $\text{Dy}_2\text{Ti}_2\text{O}_7$ , where long-range dipolar interactions between spins on the pyrochlore lattice establish the two-in–two-out ice rule (which gives the field its nondivergent character) [2], the monopoles are deconfined and interact according to a magnetic Coulomb law [3–5]. The transformation from the spin model to a Coulomb gas of magnetic monopoles simplifies the understanding of the properties of dipolar spin ices as the complicated couplings among the spins are replaced by the determinant parameters of the Coulomb gas: the elementary charge  $Q_m$ , chemical potential  $v_0$ , and hopping rate  $u$  [3,6]. Through analogs with Debye-Hückel theory of Coulomb gases, many thermodynamic observables can be conveniently calculated [7–9].

The spin relaxation rate of canonical spin ices was a particular problem in the spin representation. From high to low temperature it changes from thermally activated, to a temperature independent plateau, to a reentrant thermally

activated regime [10–13]. At high temperature, above the monopole regime, Orbach processes describe the thermally activated relaxation rate [13]. The plateau and reentrant thermally activated regimes are not readily explained in the spin representation, but can now be understood as the hopping of monopoles by quantum tunneling in screened and unscreened regimes of the Coulomb gas, respectively [11,12]. In the unscreened regime, the relaxation rate depends on the monopole density  $\rho$  with the hopping rate  $u$  as the coefficient:  $f \propto u\rho$  when the system is near equilibrium [7,8,14].

Although the monopole charge  $Q_m$  and chemical potential  $v_0$  can be calculated exactly from the spin model, the value of the monopole hopping rate  $u$  is not well understood and is usually treated as a fitting parameter [11,12,15]. For  $\text{Dy}_2\text{Ti}_2\text{O}_7$ ,  $u$  is fitted to be  $\sim 10^3$  Hz at  $T < 12$  K, which has been experimentally confirmed through the Wien effect [6]. Recently, Tomasello *et al.* found that this hopping rate can be estimated by the splitting of the crystal-electric-field (CEF) ground state doublet under an internal transverse magnetic

field of 0.1–1 T [16]. To verify the universality of this approach, it is beneficial to compare the monopole dynamics in other dipolar spin ice compounds.

The newly proposed spin ice state in the spinel  $\text{CdEr}_2\text{Se}_4$  provides such an opportunity [17–19]. In this compound,  $\text{Er}^{3+}$  ions constitute the pyrochlore lattice, and bulk measurements have revealed the Pauling entropy and local Ising character for the  $\text{Er}^{3+}$  spins [17,18]; both are strong indicators of the existence of the spin ice state although microscopic evidence is required to confirm the dipolar character necessary for deconfined, interacting monopoles. Of special importance is the low-temperature dynamics in  $\text{CdEr}_2\text{Se}_4$ , which was revealed to be 3 orders faster than that of the pyrochlore titanate  $\text{Dy}_2\text{Ti}_2\text{O}_7$  [18]. The origin of this increase and its compatibility with monopole dynamics in  $\text{CdEr}_2\text{Se}_4$  remains unclear.

In this Letter, we explore spin ice states and monopole dynamics in  $\text{CdEr}_2\text{X}_4$  ( $X = \text{Se}, \text{S}$ ). Using inelastic neutron scattering to study the CEF transitions and neutron diffuse scattering to study the spin correlations, we confirm the existence of dipolar spin ice states in  $\text{CdEr}_2\text{X}_4$ . Through ac susceptibility measurements, we reveal fast monopole dynamics in the whole quantum tunneling regime. Comparison with a calculation of the splitting of the  $\text{Er}^{3+}$  CEF ground state doublet under perturbative transverse fields reveals the increase of the monopole hopping rate as the main contribution to the fast dynamics. Thus our work explains the fast monopole dynamics in  $\text{CdEr}_2\text{X}_4$  and provides general support to this monopole hopping mechanism in dipolar spin ices.

Our powder samples of  $\text{CdEr}_2\text{Se}_4$  and  $\text{CdEr}_2\text{S}_4$  were synthesized by the solid state reaction method [20]. To reduce neutron absorption, the  $^{114}\text{Cd}$  isotope was used. X-ray diffraction measurements confirmed the good quality of our samples, with the  $\text{Er}_x\text{X}_y$  impurities being less than 1%. Inelastic neutron scattering experiments were performed on IN4 with 1.21 and 2.41 Å incident neutron wavelengths at Institut Laue-Langevin (ILL). Polarized neutron diffuse scattering experiments were performed on  $\text{CdEr}_2\text{Se}_4$  using D7 with a 4.8 Å setup at ILL. Nonpolarized neutron diffuse scattering experiments were performed on  $\text{CdEr}_2\text{S}_4$  using DMC with a 2.46 Å setup at the Swiss Spallation Neutron Source (SINQ) of the Paul Scherrer Institut (PSI). Neutron spin echo experiments were performed on IN11 at ILL. ac susceptibilities  $\chi$  in the frequency range of 1– $1 \times 10^3$  Hz were measured with the Quantum Design MPMS SQUID at the Laboratory for Scientific Developments and Novel Materials of the PSI. ac susceptibilities in the frequency range of  $2.5 \times 10^4$ – $5.5 \times 10^6$  Hz were measured using a bespoke induction ac susceptometer.

Figure 1 presents the inelastic neutron scattering results of the CEF transitions in  $\text{CdEr}_2\text{Se}_4$  and  $\text{CdEr}_2\text{S}_4$ . Altogether six peaks are observed at the base temperature for both compounds, which is consistent with the Stokes

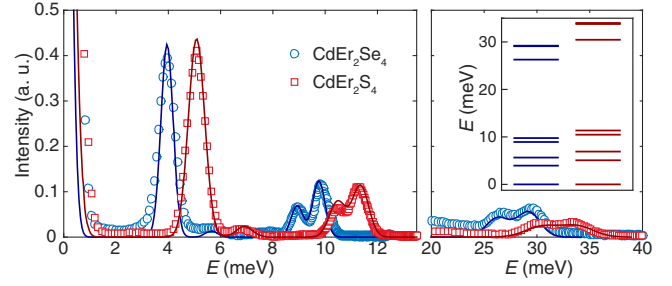


FIG. 1. Inelastic neutron scattering results of the CEF transitions in  $\text{CdEr}_2\text{Se}_4$  (measured at  $T = 2$  K) and  $\text{CdEr}_2\text{S}_4$  (measured at  $T = 1.5$  K). Error bars are smaller than the symbol size. The fits are shown as the solid lines. The inset shows the fitted energies of the CEF levels for  $\text{CdEr}_2\text{Se}_4$  (left column) and  $\text{CdEr}_2\text{S}_4$  (right column).

transitions within the  $\text{Er}^{3+} 4I_{15/2}$  manifold under  $D_{3d}$  symmetry. Using the McPhase program [21], we fitted the measured spectra with the CEF Hamiltonian  $\mathcal{H} = \sum_{lm} B_l^m \hat{O}_l^m$ , where  $\hat{O}_l^m$  are the Stevens operators and  $B_l^m$  are the corresponding coefficients. The fitting results are shown in Fig. 1 as the solid lines and Table I lists the fitted CEF parameters and ground state wave functions. The energies of the CEF levels are presented in the inset of Fig. 1, and also in Supplemental Material [20]. For both compounds, the ground states transform as the  $\Gamma_5^+ \oplus \Gamma_6^+$  dipole-octupole doublet [22,23]. Specifically, the wave functions for both of the ground state doublets are dominated by the  $|15/2, \pm 15/2\rangle$  components and have almost the same anisotropic  $g$  factors of  $g_{\perp} = 0$  and  $g_{\parallel} = 16.4$ , which is consistent with the previous report for  $\text{CdEr}_2\text{Se}_4$  [18]. Thus our inelastic neutron scattering results confirm the Ising character of the  $\text{Er}^{3+}$  spins in  $\text{CdEr}_2\text{Se}_4$  and  $\text{CdEr}_2\text{S}_4$ . Scaling our parameters [20] suggests that other members of the series may be Heisenberg-like (Dy, Yb), nonmagnetic (Tm), or Ising-like with low-lying excited states (Ho) that may be of interest for forming a quantum spin ice [24].

Although the Pauling entropy is a strong signature of the spin ice state in  $\text{CdEr}_2\text{Se}_4$  [18], it only characterizes the spin configurations at the length scale of a single tetrahedron. To realize a magnetic Coulomb gas with interacting

TABLE I. The fitted Wybourne CEF parameters (meV) and ground state doublets for  $\text{CdEr}_2\text{Se}_4$  and  $\text{CdEr}_2\text{S}_4$ .

	$B_2^0$	$B_4^0$	$B_4^3$	$B_6^0$	$B_6^3$	$B_6^6$
$\text{CdEr}_2\text{Se}_4$	-25.70	-107.73	-97.74	25.31	-19.06	9.51
$\text{CdEr}_2\text{S}_4$	-29.18	-122.72	-113.66	25.97	-21.89	14.41
$J_z$	$\pm 15/2$	$\pm 9/2$	$\pm 3/2$	$\mp 3/2$	$\mp 9/2$	
$\text{CdEr}_2\text{Se}_4$	$\pm 0.906$	0.386	$\pm 0.159$	-0.073	$\pm 0.004$	
$\text{CdEr}_2\text{S}_4$	$\pm 0.904$	0.391	$\pm 0.145$	-0.094	$\pm 0.006$	

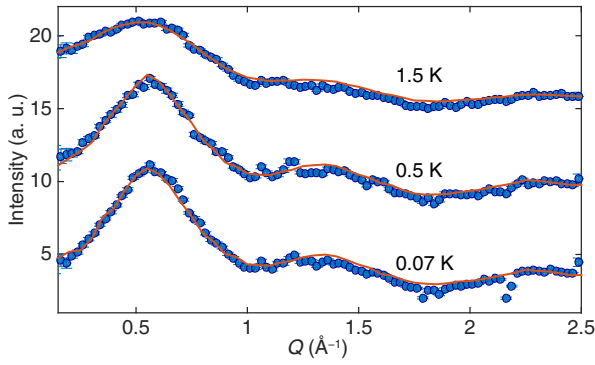


FIG. 2. CdEr<sub>2</sub>Se<sub>4</sub> magnetic scattering at 0.07, 0.5, and 1.5 K obtained from the *xyz* polarization analysis. The 0.5 (1.5) K data are shifted by 6 (12) along the *y* axis. The Monte Carlo simulation results are shown by the solid red lines.

monopoles, it is essential to have a dipolar spin ice state with power-law spin correlations, which can be verified through measurements of the spin correlations [4]. Figure 2 presents the quasistatic spin-spin correlations in CdEr<sub>2</sub>Se<sub>4</sub> obtained from polarized neutron diffuse scattering [25]. Broad peaks are observed at 0.6 and 1.4 Å<sup>-1</sup>, and the overall pattern is very similar to that of the known dipolar spin ices [26–28]. Sharp peaks with very weak intensities are also discernible near 1.1 Å<sup>-1</sup> and can be attributed to the magnetic Bragg peaks of Er<sub>x</sub>Se<sub>y</sub> impurities [20].

To fit the observed spin-spin correlations in CdEr<sub>2</sub>Se<sub>4</sub>, we performed single-spin-flip Monte Carlo simulations for the dipolar spin ice model with exchange couplings up to the second neighbors [29],

$$\mathcal{H} = J_1 \sum_{\langle ij \rangle} \sigma_i \sigma_j + J_2 \sum_{\langle\langle ij \rangle\rangle} \sigma_i \sigma_j + D r_0^3 \sum_{ij} \left[ \frac{\mathbf{n}_i \cdot \mathbf{n}_j}{|\mathbf{r}_{ij}|^3} - \frac{3(\mathbf{n}_i \cdot \mathbf{r}_{ij})(\mathbf{n}_j \cdot \mathbf{r}_{ij})}{|\mathbf{r}_{ij}|^5} \right] \sigma_i \sigma_j. \quad (1)$$

Here,  $\mathbf{n}_i$  is the unit vector along the local  $\langle 111 \rangle$  axes with the positive direction pointing from one diamond sublattice of the tetrahedra center to the other,  $\sigma_i = \pm 1$  is the corresponding Ising variable,  $J_1$  and  $J_2$  are the exchange interactions for nearest neighbors (NN)  $\langle ij \rangle$  and second-nearest neighbors  $\langle\langle ij \rangle\rangle$ , respectively,  $r_0$  is the NN distance, and  $D = \mu_0 \langle \hat{J}_z \rangle g \mu_B / (4\pi r_0^3)$  is the dipolar interaction, 0.62 and 0.69 K for CdEr<sub>2</sub>Se<sub>4</sub> and CdEr<sub>2</sub>S<sub>4</sub>, respectively. With the ALPS package [30], we implemented the Hamiltonian (1) on a  $6 \times 6 \times 6$  supercell with periodic boundary conditions. The dipolar interaction was truncated beyond the distance of three unit cells. The spin-spin correlations were evaluated every 100 sweeps during the  $4 \times 10^5$  sweeps of measurement. Assuming the effective NN coupling  $J_{\text{eff}} = J_1 + 5D/3$  to be equal to 1 K at which temperature the CdEr<sub>2</sub>Se<sub>4</sub> specific heat maximum was observed [18,31,32], we fixed  $J_1$  to  $-0.03(1)$  K and only

varied  $J_2$  in the fitting process. As is shown in Fig. 2, the model with  $J_2 = 0.04(1)$  K fits the measured spin correlations very well. We found no need to include  $J_3$ , which appears in other dipolar spin ices [29]. Although the exact value of  $J_2$  might be susceptible to both the supercell size and the dipolar cutoff, our simulations do confirm the dominance of the dipolar interactions in CdEr<sub>2</sub>Se<sub>4</sub>. Nonpolarized neutron diffuse scattering results for CdEr<sub>2</sub>S<sub>4</sub> are shown in Supplemental Material [20], which have similar  $Q$  dependence as that of CdEr<sub>2</sub>Se<sub>4</sub> and can be fitted by the dipolar spin ice model as well. In this way, we establish the existence of the dipolar spin ice state in CdEr<sub>2</sub>Se<sub>4</sub> and CdEr<sub>2</sub>S<sub>4</sub>.

With the fitted CEF ground states and coupling strengths, we can determine the monopole parameters. The monopole charge  $Q_m = 2\langle \hat{J}_z \rangle g \mu_B / \sqrt{3/2} r_0$  can be calculated to be 3.28 and 3.42  $\mu_B/\text{\AA}$  for CdEr<sub>2</sub>Se<sub>4</sub> and CdEr<sub>2</sub>S<sub>4</sub>, respectively [3]. The chemical potential  $v_0 = 2J_1 + (8/3)(1 + \sqrt{2/3})D$ , which is half of the energy cost to create and unbind a monopole-antimonopole pair [9], is 2.93 K for CdEr<sub>2</sub>Se<sub>4</sub> and 3.84 K for CdEr<sub>2</sub>S<sub>4</sub>. Although the chemical potentials in CdEr<sub>2</sub>X<sub>4</sub> are lower than that in Dy<sub>2</sub>Ti<sub>2</sub>O<sub>7</sub> (4.35 K), they are still more than two times higher than the energy cost  $E_{\text{unbind}} = (8/3)\sqrt{2/3}D$  to unbind a monopole-antimonopole pair, locating both compounds in the same weakly correlated magnetolyte regime as Dy<sub>2</sub>Ti<sub>2</sub>O<sub>7</sub> [9].

Monopole dynamics in the low and high frequency regimes can be probed with ac susceptibility [10,33–35] and neutron spin echo spectroscopy [36,37], respectively, and the representative results for CdEr<sub>2</sub>Se<sub>4</sub> are shown in Figs. 3(a) and 3(b). Figure 3(c) summarizes the temperature dependence of the characteristic relaxation time  $\tau = 1/2\pi f$  in CdEr<sub>2</sub>X<sub>4</sub>, where the results for  $\tau > 1 \times 10^{-3}$  s are extracted from the peak positions of the imaginary part of the ac susceptibility  $\chi''(T)$ , the results for  $10^{-5} > \tau > 10^{-7}$  s are obtained by fitting  $\chi(\omega)$  to the Cole-Cole model [38], and the results for  $\tau < 10^{-8}$  s are obtained by fitting the neutron spin echo intermediate scattering function with  $S(Q, t)/S(Q, 0) = A \exp[-t/\tau(T)]$  [36,37]. The relaxation time in Dy<sub>2</sub>Ti<sub>2</sub>O<sub>7</sub> [33,34] is also shown in Fig. 3(c) for comparison.

First, we observe that at  $T > 10$  K, the relaxation time in CdEr<sub>2</sub>X<sub>4</sub> obeys the Orbach law of  $\tau = \tau_0 [\exp(\Delta/k_B T) - 1]$  [13], with the parameters  $\tau_0 = 3.93(9) \times 10^{-11}$  s and  $\Delta = 77.1$  K for CdEr<sub>2</sub>Se<sub>4</sub>, and  $\tau_0 = 2.73(5) \times 10^{-11}$  s and  $\Delta = 96.3$  K for CdEr<sub>2</sub>S<sub>4</sub>. The fitted excitation energies  $\Delta$  in CdEr<sub>2</sub>X<sub>4</sub> are much smaller than that of Dy<sub>2</sub>Ti<sub>2</sub>O<sub>7</sub> ( $\Delta > 230$  K), which is due to their lower CEF excited states [13].

The Orbach behavior of the relaxation rate does not extend to the lowest temperature. Instead, at  $T$  in between 2 and 5 K, a plateau region with  $\tau \sim 4.9 \times 10^{-7}$  s, which was inaccessible in the previous susceptibility measurements

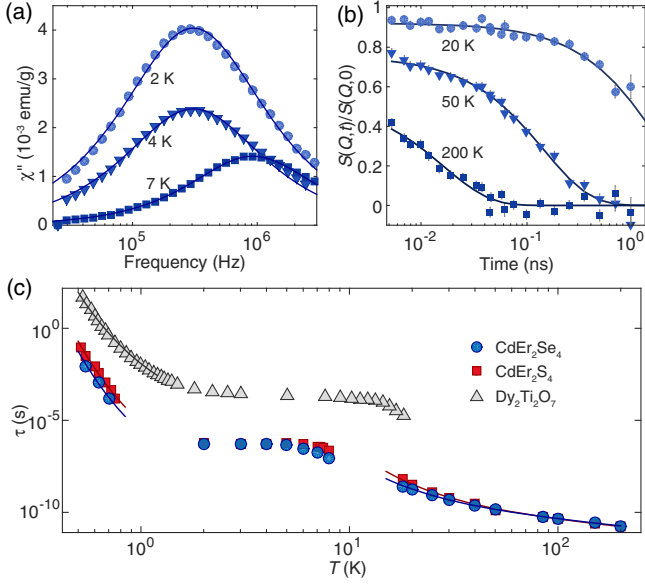


FIG. 3. (a) Imaginary parts of the ac susceptibilities of CdEr<sub>2</sub>Se<sub>4</sub> measured at 2, 4, and 7 K with the Cole-Cole model fits shown as the solid lines. (b) Normalized spin echo intermediate scattering function  $S(Q, t)/S(Q, 0)$  of CdEr<sub>2</sub>Se<sub>4</sub> measured at 20, 50, and 200 K with the fits shown as the solid lines. (c) Extracted relaxation time in CdEr<sub>2</sub>Se<sub>4</sub> and CdEr<sub>2</sub>S<sub>4</sub>. Error bars are smaller than the symbol sizes. The Arrhenius (Orbach) fits in the low (high) temperature regime are shown as the solid lines. Relaxation rates together with the low-temperature Arrhenius fit for Dy<sub>2</sub>Ti<sub>2</sub>O<sub>7</sub> [33,34] are shown for comparison.

[18], is observed for both CdEr<sub>2</sub>Se<sub>4</sub> and CdEr<sub>2</sub>S<sub>4</sub>, reminiscent of the  $\tau \sim 2.6 \times 10^{-4}$  s quantum tunneling plateau in Dy<sub>2</sub>Ti<sub>2</sub>O<sub>7</sub> [10,11,34]. Such a similarity extends to even lower temperatures where the relaxation time starts rising again. As can be seen in Fig. 3(c), at  $T < 1$  K, the relaxation time in CdEr<sub>2</sub>X<sub>4</sub> can be described by the Arrhenius law of  $\tau_0 \exp(\Delta/k_B T)$ , with parameters  $\tau_0 = 1.01(1) \times 10^{-10}$  s and  $\Delta = 10.07$  K for CdEr<sub>2</sub>Se<sub>4</sub>, and  $\tau_0 = 2.9(1) \times 10^{-10}$  s and  $\Delta = 10.2(6)$  K for CdEr<sub>2</sub>S<sub>4</sub>. Because of the limited data points for CdEr<sub>2</sub>Se<sub>4</sub>, the fitted  $\Delta$  value from Ref. [18] has been used. The activation energies in CdEr<sub>2</sub>X<sub>4</sub> are very close to that of Dy<sub>2</sub>Ti<sub>2</sub>O<sub>7</sub>, where the Arrhenius law with  $\tau_0 = 3.07 \times 10^{-7}$  s and  $\Delta = 9.93$  K has been observed in a similar temperature regime [33].

Despite the similar temperature evolution, the absolute values of the monopole relaxation rates in CdEr<sub>2</sub>X<sub>4</sub> are about  $10^3$  times higher than that in Dy<sub>2</sub>Ti<sub>2</sub>O<sub>7</sub> for the whole measured quantum tunneling region, which cannot be simply accounted for by the difference of the monopole densities  $\rho$ . Assuming  $\rho(T) \propto \exp(-v_0/k_B T)$ , the monopole densities in CdEr<sub>2</sub>X<sub>4</sub> are no more than 10 times higher than that of Dy<sub>2</sub>Ti<sub>2</sub>O<sub>7</sub> in the investigated quantum tunneling region. According to the  $f \propto u\rho$  relation of the Debye-Hückel theory, there must be a 2 orders increase of the monopole hopping rates  $u$  in CdEr<sub>2</sub>X<sub>4</sub>.

Following Tomasello *et al.* [16], we analyze the perturbation effect of an internal transverse magnetic field on the CEF ground state doublet in CdEr<sub>2</sub>Se<sub>4</sub> and CdEr<sub>2</sub>S<sub>4</sub>. Because of the similar NN couplings [9], we expect similar internal field strengths in CdEr<sub>2</sub>X<sub>4</sub> and Dy<sub>2</sub>Ti<sub>2</sub>O<sub>7</sub> [39]. The perturbed Hamiltonian can be written as

$$\mathcal{H} = \sum_{lm} B_l^m \hat{O}_l^m + H \cos(\phi) \hat{J}_x + H \sin(\phi) \hat{J}_y, \quad (2)$$

where the  $y$  direction is along the  $C_2$  axis and  $\phi$  is the angle between the transverse field  $H$  and the  $x$  direction (see the inset of Fig. 4). Similar to the Dy<sup>3+</sup> ions in Dy<sub>2</sub>Ti<sub>2</sub>O<sub>7</sub> [16], the Kramers degeneracy of the Er<sup>3+</sup> ions causes a third-order dependence of the ground state splitting on the field strength in the perturbative regime:  $\Delta E = \alpha[1 + A \cos(6\phi)]H^3$ . Using the McPhase program [21], we directly diagonalize the Hamiltonian (2) and fit the coefficients to be  $\alpha = 2.80 \times 10^{-4}$  ( $1.95 \times 10^{-4}$ ) [meV/T<sup>3</sup>] and  $A = 0.136$  (0.098) for CdEr<sub>2</sub>Se<sub>4</sub> (CdEr<sub>2</sub>S<sub>4</sub>). For Dy<sub>2</sub>Ti<sub>2</sub>O<sub>7</sub>, using the CEF parameters of Ref. [40], the coefficients are calculated to be  $\alpha = 2.14 \times 10^{-6}$  [meV/T<sup>3</sup>] and  $A = 0.183$ . As is compared in Fig. 4 for magnetic field along the  $x$  direction, the CEF ground state splittings in CdEr<sub>2</sub>X<sub>4</sub> are indeed  $\sim 10^2$  larger than that in Dy<sub>2</sub>Ti<sub>2</sub>O<sub>7</sub> under the same transverse magnetic field. This higher susceptibility to transverse magnetic field is a property of the full CEF Hamiltonian of CdEr<sub>2</sub>X<sub>2</sub> as compared to that of Dy<sub>2</sub>Ti<sub>2</sub>O<sub>7</sub>.

Our results suggest that to explain the much faster dynamics of CdEr<sub>2</sub>X<sub>4</sub> vs Dy<sub>2</sub>Ti<sub>2</sub>O<sub>7</sub> only similar monopole populations combined with a much faster monopole hopping rate in the former are required, and also support the single-ion quantum tunneling process proposed in Ref. [16] as a general monopole hopping mechanism in dipolar spin ices. Meanwhile, it should be noted that other factors may also contribute to the high monopole hopping rates in CdEr<sub>2</sub>X<sub>4</sub>. For example, the nonvanishing components of  $|J_x J_z\rangle$  with  $|J_z| \leq 7/2$  in CdEr<sub>2</sub>X<sub>4</sub> ground state doublet might induce multipolar interactions that can further increase the monopole hopping rates [41].

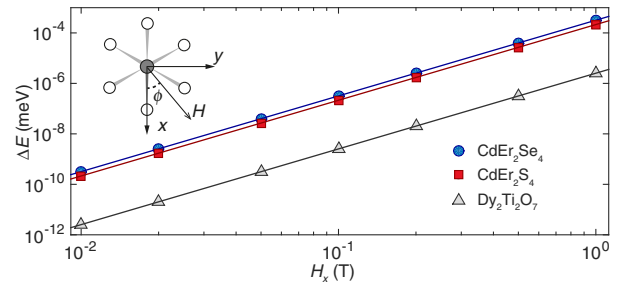


FIG. 4. Splittings of the CEF ground state doublet in CdEr<sub>2</sub>Se<sub>4</sub>, CdEr<sub>2</sub>S<sub>4</sub>, and Dy<sub>2</sub>Ti<sub>2</sub>O<sub>7</sub> under a perturbative magnetic field along the  $x$  direction. Definitions of the axes are shown in the inset.

In summary, neutron scattering investigations of the spin correlations in  $\text{CdEr}_2\text{X}_4$  ( $X = \text{Se}, \text{S}$ ) confirm they are the first spinels that realize dipolar spin ice states. High-temperature Orbach behavior gives way to fast (compared to  $\text{Dy}_2\text{Ti}_2\text{O}_7$ ) monopole hopping dynamics at low temperature. Comparison of monopole populations calculated using Coulomb gas parameters estimated from the diffuse scattering experiments and bulk properties, and monopole hopping rates calculated using the CEF Hamiltonian derived from our inelastic neutron scattering data, show that the main contribution to the fast monopole dynamics of  $\text{CdEr}_2\text{X}_4$  is due to the much larger hopping rate. The reproduction of the very different relaxation rates in  $\text{CdEr}_2\text{X}_4$  and  $\text{Dy}_2\text{Ti}_2\text{O}_7$  using realistic parameters supports the general application of this method to the description of monopole hopping processes in dipolar spin ices.

$\text{CdR}_2\text{X}_4$  (and  $\text{MgR}_2\text{X}_4$  [19]) afford new possibilities in the study of frustrated magnetism on the pyrochlore lattice, with single-ion ground states [20], interactions, and dynamics that contrast with the well-known pyrochlore oxides [42]. One immediate benefit of the fast monopole hopping rate in  $\text{CdEr}_2\text{X}_4$  is that it enables the study of the magnetic Coulomb phase in a broader frequency regime. In particular, nonequilibrium phenomena such as the Wien effect [14,43], which appear in  $\text{Dy}_2\text{Ti}_2\text{O}_7$  at temperatures well below those measured here (by susceptibility), may be modified. On the other hand, if the timescale of dynamics is taken as a measure of the quantum contribution to the dynamics of a spin ice, going from slow and classical ( $\text{Dy}_2\text{Ti}_2\text{O}_7$ ) to fast and quantum (e.g., Tb- or Pr-based quantum spin ice candidates [44]),  $\text{CdEr}_2\text{X}_4$  offer an intermediate case that may help in the extrapolation of our understanding of the former to that of the latter. Finally,  $\text{CdEr}_2\text{X}_4$  offer the possibility to look for a new ground state of dipolar spin ice [45]. As is discussed in Supplemental Material [20], for  $\text{Dy}_2\text{Ti}_2\text{O}_7$ , an antiferromagnetic ordering transition at  $\sim 0.1$  K is expected [45–48], but is experimentally inaccessible due to the relatively high freezing temperature of  $\sim 0.65$  K [10,49]. For  $\text{CdEr}_2\text{Se}_4$ , our parameters predict a ferromagnetic ordering transition at  $\sim 0.37$  K and a comparable freezing temperature of  $\sim 0.29$  K [20]. This means that both the ferromagnetic ground state and new monopole interactions caused by the bandwidth of the spin ice states may be experimentally accessible [20]. Further dynamical and thermodynamic measurements at low temperatures would be required to conclude whether the spin ice state that we observed at 0.07 K is an equilibrium state and to explore the possible ordering transition in  $\text{CdEr}_2\text{X}_4$ .

We acknowledge valuable discussions with C. Castelnovo, M. J. P. Gingras, B. Tomasello, L. D. C. Jaubert, H. Kadowaki, G. Chen, M. Ruminy, J. Xu, J. S. White, A. Turrini, and J.-H. Chen. We thank V. Markushin for help with the Merlin4 cluster. Our neutron scattering experiments were performed at the ILL, Grenoble, France,

and the Swiss Spallation Neutron Source SINQ, PSI, Villigen, Switzerland. The susceptibility measurements were carried out in the Laboratory for Scientific Developments and Novel Materials of the PSI. The Monte Carlo simulations were performed on the Merlin4 cluster at the PSI. This work was supported by the Swiss National Science Foundation (Grants No. 20021-140862 and No. 20020-162626, SCOPES Grant No. IZ73Z0-152734/1). S. R. G. thanks EPSRC for financial support under Grant No. EP/L019760/1. V. T. and A. L. acknowledge funding from the Deutsche Forschungsgemeinschaft (DFG) via the Transregional Collaborative Research Center TRR 80. E. C. acknowledges support from the Danish Research Council for Science and Nature through DANSCATT.

\*oksana.zaharko@psi.ch

†tom.fennell@psi.ch

- [1] C. L. Henley, *Annu. Rev. Condens. Matter Phys.* **1**, 179 (2010).
- [2] S. T. Bramwell and M. J. P. Gingras, *Science* **294**, 1495 (2001).
- [3] C. Castelnovo, R. Moessner, and S. L. Sondhi, *Nature (London)* **451**, 42 (2008).
- [4] T. Fennell, P. P. Deen, A. R. Wildes, K. Schmalzl, D. Prabhakaran, A. T. Boothroyd, R. J. Aldus, D. F. McMorrow, and S. T. Bramwell, *Science* **326**, 415 (2009).
- [5] D. J. P. Morris, D. A. Tennant, S. A. Grigera, B. Klemke, C. Castelnovo, R. Moessner, C. Czternasty, M. Meissner, K. C. Rule, J.-U. Hoffmann, K. Kiefer, S. Gerischer, D. Slobinsky, and R. S. Perry, *Science* **326**, 411 (2009).
- [6] S. R. Giblin, S. T. Bramwell, P. C. W. Holdsworth, D. Prabhakaran, and I. Terry, *Nat. Phys.* **7**, 252 (2011).
- [7] I. A. Ryzhkin, *J. Exp. Theor. Phys.* **101**, 481 (2005).
- [8] C. Castelnovo, R. Moessner, and S. L. Sondhi, *Phys. Rev. B* **84**, 144435 (2011).
- [9] H. D. Zhou, S. T. Bramwell, J. G. Cheng, C. R. Wiebe, G. Li, L. Balicas, J. A. Bloxson, H. J. Silverstein, J. S. Zhou, J. B. Goodenough, and J. S. Gardner, *Nat. Commun.* **2**, 478 (2011).
- [10] J. Snyder, B. G. Ueland, J. S. Slusky, H. Karunadasa, R. J. Cava, and P. Schiffer, *Phys. Rev. B* **69**, 064414 (2004).
- [11] L. D. C. Jaubert and P. C. W. Holdsworth, *Nat. Phys.* **5**, 258 (2009).
- [12] L. D. C. Jaubert and P. C. W. Holdsworth, *J. Phys. Condens. Matter* **23**, 164222 (2011).
- [13] M. Ruminy, S. Chi, S. Calder, and T. Fennell, *Phys. Rev. B* **95**, 060414 (2017).
- [14] C. Paulsen, M. J. Jackson, E. Lhotel, B. Canals, D. Prabhakaran, K. Matsuhira, S. R. Giblin, and S. T. Bramwell, *Nat. Phys.* **10**, 135 (2014).
- [15] H. Takatsu, K. Goto, H. Otsuka, R. Higashinaka, K. Matsubayashi, Y. Uwatoko, and H. Kadowaki, *J. Phys. Soc. Jpn.* **82**, 104710 (2013).
- [16] B. Tomasello, C. Castelnovo, R. Moessner, and J. Quintanilla, *Phys. Rev. B* **92**, 155120 (2015).
- [17] G. C. Lau, R. S. Freitas, B. G. Ueland, P. Schiffer, and R. J. Cava, *Phys. Rev. B* **72**, 054411 (2005).

- [18] J. Lago, I. Živković, B. Z. Malkin, J. R. Fernandez, P. Ghigna, P. D. de Réotier, A. Yaouanc, and T. Rojo, *Phys. Rev. Lett.* **104**, 247203 (2010).
- [19] D. Reig-i Plessis, S. V. Geldern, A. A. Aczel, and G. J. MacDougall, [arXiv:1703.04267](https://arxiv.org/abs/1703.04267).
- [20] See Supplemental Material at <http://link.aps.org/supplemental/10.1103/PhysRevLett.120.137201> for details on the sample preparation, impurities in  $\text{CdEr}_2\text{Se}_4$ , CEF levels in  $\text{CdEr}_2\text{X}_4$  and  $\text{CdR}_2\text{X}_4$ , spin correlations in  $\text{CdEr}_2\text{S}_4$ , and estimates of ordering and freezing temperatures in  $\text{CdEr}_2\text{Se}_4$ .
- [21] M. Rotter, *J. Magn. Mater.* **272–276**, E481 (2004).
- [22] Y.-P. Huang, G. Chen, and M. Hermele, *Phys. Rev. Lett.* **112**, 167203 (2014).
- [23] Y.-D. Li, X. Wang, and G. Chen, *Phys. Rev. B* **94**, 201114 (2016).
- [24] H. R. Molavian, M. J. P. Gingras, and B. Canals, *Phys. Rev. Lett.* **98**, 157204 (2007).
- [25] G. Ehlers, J. R. Stewart, A. R. Wildes, P. P. Deen, and K. H. Andersen, *Rev. Sci. Instrum.* **84**, 093901 (2013).
- [26] H. Kadowaki, Y. Ishii, K. Matsuhira, and Y. Hinatsu, *Phys. Rev. B* **65**, 144421 (2002).
- [27] I. Mirebeau and I. Goncharenko, *J. Phys. Condens. Matter* **16**, S653 (2004).
- [28] A. M. Hallas, J. A. M. Paddison, H. J. Silverstein, A. L. Goodwin, J. R. Stewart, A. R. Wildes, J. G. Cheng, J. S. Zhou, J. B. Goodenough, E. S. Choi, G. Ehlers, J. S. Gardner, C. R. Wiebe, and H. D. Zhou, *Phys. Rev. B* **86**, 134431 (2012).
- [29] T. Yavors’kii, T. Fennell, M. J. P. Gingras, and S. T. Bramwell, *Phys. Rev. Lett.* **101**, 037204 (2008).
- [30] B. Bauer, L. D. Carr, H. G. Evertz, A. Feiguin, J. Freire, S. Fuchs, L. Gamper, J. Gukelberger, E. Gull, S. Guertler, A. Hehn, R. Igarashi, S. V. Isakov, D. Koop, P. N. Ma, P. Mates, H. Matsuo, O. Parcollet, G. Pawłowski, J. D. Picon *et al.*, *J. Stat. Mech.* **2011**, P05001 (2011).
- [31] B. C. den Hertog and M. J. P. Gingras, *Phys. Rev. Lett.* **84**, 3430 (2000).
- [32] H. D. Zhou, J. G. Cheng, A. M. Hallas, C. R. Wiebe, G. Li, L. Balicas, J. S. Zhou, J. B. Goodenough, J. S. Gardner, and E. S. Choi, *Phys. Rev. Lett.* **108**, 207206 (2012).
- [33] L. R. Yaraskavitch, H. M. Revell, S. Meng, K. A. Ross, H. M. L. Noad, H. A. Dabkowska, B. D. Gaulin, and J. B. Kycia, *Phys. Rev. B* **85**, 020410 (2012).
- [34] K. Matsuhira, Y. Hinatsu, and T. Sakakibara, *J. Phys. Condens. Matter* **13**, L737 (2001).
- [35] J. A. Quilliam, L. R. Yaraskavitch, H. A. Dabkowska, B. D. Gaulin, and J. B. Kycia, *Phys. Rev. B* **83**, 094424 (2011).
- [36] G. Ehlers, A. L. Cornelius, M. Orendác, M. Kajnaková, T. Fennell, S. T. Bramwell, and J. S. Gardner, *J. Phys. Condens. Matter* **15**, L9 (2003).
- [37] G. Ehlers, A. L. Cornelius, T. Fennell, M. Koza, S. T. Bramwell, and J. S. Gardner, *J. Phys. Condens. Matter* **16**, S635 (2004).
- [38] L. Bovo, J. A. Bloxsom, D. Prabhakaran, G. Aeppli, and S. T. Bramwell, *Nat. Commun.* **4**, 1535 (2013).
- [39] G. Sala, C. Castelnovo, R. Moessner, S. L. Sondhi, K. Kitagawa, M. Takigawa, R. Higashinaka, and Y. Maeno, *Phys. Rev. Lett.* **108**, 217203 (2012).
- [40] M. Ruminy, E. Pomjakushina, K. Iida, K. Kamazawa, D. T. Adroja, U. Stuhr, and T. Fennell, *Phys. Rev. B* **94**, 024430 (2016).
- [41] J. G. Rau and M. J. P. Gingras, *Phys. Rev. B* **92**, 144417 (2015).
- [42] J. S. Gardner, M. J. P. Gingras, and J. E. Greedan, *Rev. Mod. Phys.* **82**, 53 (2010).
- [43] C. Paulsen, S. R. Giblin, E. Lhotel, D. Prabhakaran, G. Balakrishnan, K. Matsuhira, and S. T. Bramwell, *Nat. Phys.* **12**, 661 (2016).
- [44] M. J. P. Gingras and P. A. McClarty, *Rep. Prog. Phys.* **77**, 056501 (2014).
- [45] P. A. McClarty, O. Sikora, R. Moessner, K. Penc, F. Pollmann, and N. Shannon, *Phys. Rev. B* **92**, 094418 (2015).
- [46] R. G. Melko, B. C. den Hertog, and M. J. P. Gingras, *Phys. Rev. Lett.* **87**, 067203 (2001).
- [47] J. P. C. Ruff, R. G. Melko, and M. J. P. Gingras, *Phys. Rev. Lett.* **95**, 097202 (2005).
- [48] P. Henelius, T. Lin, M. Enjalran, Z. Hao, J. G. Rau, J. Altosaar, F. Flicker, T. Yavors’kii, and M. J. P. Gingras, *Phys. Rev. B* **93**, 024402 (2016).
- [49] D. Pomaranski, L. R. Yaraskavitch, S. Meng, K. A. Ross, H. M. L. Noad, H. A. Dabkowska, B. D. Gaulin, and J. B. Kycia, *Nat. Phys.* **9**, 353 (2013).